
Constrained Optimization for Training Deep Neural Networks Under Class Imbalance

Sara Sangalli¹ Ertunc Erdil¹ Andreas Hoetker² Olivio Donati² Ender Konukoglu¹

Abstract

Deep neural networks (DNNs) are notorious for making more mistakes for the classes that have substantially fewer samples than the others during training. Such class imbalance is ubiquitous in clinical applications and very crucial to handle because the classes with fewer samples most often correspond to critical cases (e.g., cancer) where misclassifications can have severe consequences. Not to miss such cases, binary classifiers need to be operated at high True Positive Rates (TPR) by setting a higher threshold but this comes at the cost of very high False Positive Rates (FPR) for problems with class imbalance. Existing methods for learning under class imbalance most often do not take this into account. We argue that prediction accuracy should be improved by emphasizing reducing FPRs at high TPRs for problems where misclassification of the positive samples are associated with higher cost. To this end, we pose the training of a DNN for binary classification as a constrained optimization problem and introduce a novel constraint that can be used with existing loss functions to enforce maximal area under the ROC curve (AUC). We solve the resulting constrained optimization problem using an Augmented Lagrangian method (ALM), where the constraint emphasizes reduction of FPR at high TPR. We present experimental results for image-based classification applications using the CIFAR10 and an in-house medical imaging dataset. Our results demonstrate that the proposed method almost always improves the loss functions it is used with by attaining lower FPR at high TPR and higher or equal AUC.¹

¹Department of Electrical Engineering and Information Technology, ETH Zürich, Zürich, Switzerland

²Institute of Diagnostic and Interventional Radiology of Universitätsspital Zürich

Correspondence to: Sara Sangalli <sansara@student.ethz.ch>.

¹Code available at <https://gitlab.ethz.ch/sansara/alm-dnn>.

1. Introduction

Deep Neural Networks (DNNs) perform extremely well in many classification tasks when sufficiently large and representative datasets are available for training. However, in many real world applications, it is not uncommon to encounter highly-skewed class distributions, i.e., majority of the data belong to only a few classes while some classes are represented with scarce instances. Training DNNs on such imbalanced datasets leads to models that are biased toward majority classes with poor prediction accuracy for the minority class samples. While this is problematic for all such applications, it poses an even greater issue for “critical” applications where misclassifying samples belonging to the minority class can have severe consequences. One domain where such applications are common and machine learning is having an important impact is medical imaging.

In medical imaging, applications with data imbalance are ubiquitous (Litjens et al., 2017) and cost of making some types of mistakes are more severe than others. For instance, in a diagnosis application, discarding a cancer case as healthy (False Negative) is more costly than classifying a healthy subject as having cancer (False Positive). While the latter creates burden for the subject as well as health-care system through additional tests that may be invasive and expensive, the former, i.e., failure to identify a cancerous case, would delay the diagnosis and jeopardise treatment success. In such applications, binary classifiers are operated at high True Positive Rates (TPR) even when this means having higher False Positive Rates (FPR). To make matters more complicated, there are usually significantly fewer samples to represent cases where mistakes are more severe. For instance, in (Djavan et al., 2000) authors found out that only 30% of even the most suspicious cases identified with initial testing actually have prostate cancer. This class imbalance increases the FPR even higher in “critical” applications because the models tend to misclassify minority classes more often.

While various methods for learning with imbalanced datasets exist, to the best of our knowledge, these methods do not take into account the fact that “critical” applications need to be operated at high TPR. We believe that for such applications ensuring low FPR at high TPR should be the

main goal to make binary classifiers useful in practice. This motivates us to design a new strategy for training DNNs for binary classification.

Contribution: In this paper, we pose the training of a DNN for binary classification under class imbalance as a constrained optimization problem and propose a novel constraint that can be used with existing loss functions. We define the constraint using Mann-Whitney statistics (Mann & Whitney, 1947) in order to maximize the AUC, but in an asymmetric way to favor reduction of false positives at high true positive (or low false negative) rates. Then, we transfer the constrained problem to its dual unconstrained optimization problem using an Augmented Lagrangian method (ALM) (Bertsekas, 1999). We optimize the resulting loss function using stochastic gradient descent. Unlike the existing methods that directly optimizes AUC, we incorporate AUC optimization in a principled way into a constrained optimization framework.

Parameter initialization is crucial when using ALM even if the model has only a few parameters (Hestenes, 1969) due to the many terms involved in the loss function. This is even more crucial for DNNs where the number of parameters are quite high. We tackle this problem by a simple two steps strategy: 1) we pre-train DNNs using a conventional loss function starting from a random initialization until convergence, 2) we further optimize the pre-trained models using the proposed constraint added to the loss function.

We present an extensive evaluation of the proposed method for image-based binary classification on two datasets: 1) an in-house medical dataset for prostate cancer, 2) a publicly available computer vision dataset, CIFAR10 (Krizhevsky et al., 2009), for reproducibility purposes. In both datasets, we performed experiments by simulating different class imbalance ratios. In our experiments, we applied the proposed method on DNNs that are pre-trained with 8 different loss functions for classification, most of which were proposed to handle class imbalance, and compare the results with the pre-trained baselines. We also compare our results with an existing method that directly optimizes AUC to demonstrate the benefit of putting AUC as a constraint.

The remaining of the paper is organized as follows. In Sec. 2 we present existing methods that are proposed to handle class imbalance. Sec. 3 is devoted to background that is useful for understanding the proposed method. In Sec. 5, we present our experimental results. We conclude in Sec. 6.

2. Related work

2.1. Class imbalance

Various methods have already been proposed to learn better models with class imbalanced datasets. We group the

existing methods into three classes: sampling-based, cost sensitive training-based and classifier-based methods.

Sampling-based methods: Methods in this group aims to deal with the data imbalance problem by generating a balanced distribution through getting more samples from the minority class or less samples from the majority class. A simple approach of replicating a certain number of minority class instances can lead to models that are over-fitting to the over-sampled instances. Chawla et al. (2002) propose to generate novel minority class samples by interpolating the neighboring data points. Haibo He et al. (2008) extends (Chawla et al., 2002) by proposing a way to estimate the number of minority class samples to be synthesized. Drummond et al. (2003) approaches the problem from the opposite perspective and randomly under-sample majority class instances instead of synthesizing new data for the minority class. Despite the fact that losing valuable information for the majority class, Drummond et al. (2003) report that it leads to better results compared to the former approaches. Although, these earlier sampling-based methods are useful for the low dimensional data, they suffer from issues in higher dimensions, e.g. images, since interpolation does not lead to realistic samples. Moreover, they still suffer from generalization difficulties (He & Garcia, 2009). Sham-solmoali et al. (2020) propose to use adversarial training with capsule networks to generate more realistic samples for the minority classes, and demonstrate its effectiveness for class imbalance. More recently, Liu et al. (2020) propose a method which adaptively samples a subset from the training set in each iteration to train multiple classifiers which are then ensembled for prediction.

Cost sensitive training-based methods: This family of methods aim handling class imbalance by designing an appropriate loss function to be used during training. In particular, they design the loss functions to give more emphasis to the minority class samples, or the class with higher associated risk, than the majority ones during training (Thai-Nghe et al., 2010). Zadrozny et al. (2003) propose a loss function, which we refer to as Weighted BCE (W-BCE), where minority class samples are multiplied by a constant to introduce more cost to misclassification of those samples. Huang et al. (2016) propose a method function that aims to learn more discriminative latent representations by enforcing DNNs to maintain inter-cluster and inter-class margins where clusters are formed using k-means clustering. They demonstrate that the tighter constraint inherently reduces class imbalance. In a more recent work, Cui et al. (2019) propose a loss function called class-balanced binary cross-entropy (CB-BCE) to weight BCE inversely proportionally to the class frequencies to amplify the loss for the minority class samples. In a similar vein, Lin et al. (2017) modifies BCE and propose symmetric focal loss (S-FL) by multiplying it with the inverse of the prediction probability to introduce

more cost to the samples that DNNs are not very confident. Liu et al. (2016) introduces symmetric margin loss (S-ML) by introducing a margin to the BCE loss. Li et al. (2019) investigate different loss functions such as S-FL and S-ML, and propose their asymmetric versions, A-FL and A-ML, by introducing a margin for the minority class samples to handle class imbalance. In a different line of work, Wang et al. (2016) propose a method called mean squared false error (MSFE) by performing simple yet effective modification to the mean squared error (MSE) loss. Unlike MSE, which computes an average error from all samples without considering their classes, MSFE computes a mean error for each sample and averages them.

A particular group within the cost sensitive training-based methods focus on optimizing AUC and our method falls into this group. AUC optimization is an ideal choice for class imbalance since AUC is not sensitive to class distributions (Cortes & Mohri, 2004). Rakotomamonjy (2004) proposes a support vector machine (SVM) based loss function that maximizes AUC and demonstrate its effectiveness for the class imbalance. Zhao et al. (2011) approach the class imbalance problem from online learning perspective and propose an AUC optimization-based loss function. Gao et al. (2013) proposes a one-pass method for AUC optimization that does not require storing data unlike the previous online methods. Another online AUC optimization method proposed by Ying et al. (2016) represent AUC optimization as a convex-concave saddle point problem and propose a method that has time and space complexity of a single data point. Despite their usefulness, all aforementioned AUC optimization-based methods were applied to linear predictive models and their performance on DNNs are unknown. Sulam et al. (2017) applies online AUC optimization on a small dataset for breast cancer detection where they also mention that extension to larger datasets is not feasible. In a very recent work called mini-batch AUC (MBAUC), Gul-tekin et al. (2020) extend AUC optimization to non-linear models with DNNs by optimizing AUC with minibatches and demonstrate its effectiveness on various datasets.

Classifier-based methods: Methods from this category operate in test time and are mostly based on thresholding and scaling the output class probabilities. One common approach is to divide the output for each class by their prior probabilities which shown to be effective to handle class imbalance in both classification (Lawrence et al., 1996; Buda et al., 2018) and semantic segmentation (Chan et al., 2019). In a recent work, Tian et al. (2020) argue that the previous methods from this family suffer from diminished overall accuracy despite the improved detection on minority classes. They mitigate this problem by proposing a method re-balancing the posterior in test-time.

The proposed constrained optimization method differs from

existing works in that it enforces maximal AUC as a constraint in a way that favors reducing FPR at high TPR and can be used with existing loss functions.

3. Background

3.1. Augmented Lagrangian method (ALM)

A generic optimization problem for an objective function $F(\theta)$ subject to the constraints $\mathcal{C}(\theta) = \{c_1(\theta), \dots, c_m(\theta)\}$ can be expressed as (Bertsekas, 1999; Nocedal & Wright, 2006):

$$\begin{aligned} & \arg \min_{\theta} F(\theta) \\ & \text{subject to } \mathcal{C}(\theta), \quad \theta \in \Theta \end{aligned} \quad (1)$$

One of the earlier methods, quadratic penalty method (Bertsekas, 1976), converts the constrained optimization problem in Eq. (1) to an unconstrained optimization problem by adding the constraint to the objective function as a quadratic penalty term:

$$\arg \min_{\theta \in \Theta} F(\theta) + \mu \sum_{i=1}^m \|c_i(\theta)\|^2 \quad (2)$$

where μ is a positive parameter which controls the contribution of the penalty term to the overall loss function. Increasing μ indefinitely over the iterations is necessary to convexify the loss and ensure convergence. However, as the μ increases, the penalty term prevails $F(\theta)$, which makes training unstable (Bertsekas, 1976).

The method of Lagrange multipliers converts Eq. (1) into the unconstrained optimization problem by adding the constraints to the objective function as follows:

$$\mathcal{L}(\theta, \lambda) = F(\theta) + \sum_{i=1}^m \lambda_i c_i(\theta) \quad (3)$$

where λ are called as Lagrange multipliers. The method of Lagrange multipliers deals with the instability of quadratic penalty method, however, it requires the objective function to be convex which is a drawback.

Augmented Lagrangian Methods (or methods of multipliers) overcome the limitations of the above-mentioned two approaches. Here, the penalty concept is merged with the primal-dual philosophy of classic Lagrangian function. In such methods, the penalty term is added not to the objective function $F(\theta)$ but rather to its Lagrangian function, thus forming the Augmented Lagrangian Function:

$$\mathcal{L}_{\mu}(\theta, \lambda) = F(\theta) + \mu \sum_{i=1}^m \|c_i(\theta)\|^2 + \sum_{i=1}^m \lambda_i c_i(\theta) \quad (4)$$

In practice, this method consists of iteratively solving a sequence of problems as:

$$\max_{\lambda^k} \min_{\theta} \mathcal{L}_{\mu^k}(\theta, \lambda^k), \quad \theta \in \Theta \quad (5)$$

Where $\{\lambda^k\}$ is a bounded sequence in \mathcal{R}^m , updated as $\lambda_i^{k+1} = \lambda_i^k + \mu c_i(\theta)$. $\{\mu^k\}$ is a positive penalty parameter sequence, with $0 < \mu^k \leq \mu^{k+1}$, $\mu^k \rightarrow \infty$, which may be either pre-selected or generated during the computation according to a defined scheme. In ALM, increasing μ^k to indefinitely is not necessary as in the quadratic penalty method. Thus, it does not suffer from training instabilities due to the constraint prevailing $F(\theta)$. Furthermore, it does not require convexity assumption as in the method of Lagrange multipliers to ensure convergence (Bertsekas, 1976).

3.2. Area under the ROC curve (AUC), TPR and FPR

AUC is a performance evaluation metric that is widely used in binary classification problems. It is a threshold-independent method which measures the separability of two classes at various thresholds. AUC is also defined as the probability of a random positive sample taking a value higher than a random negative sample (Hanley & Mcneil, 1982). More formally, let y_1^+, \dots, y_m^+ be the outputs of a classifier on positive examples and y_1^-, \dots, y_n^- be the outputs on negative ones. Then an unbiased estimator of the AUC is

$$AUC = \frac{\sum_{i=1}^m \sum_{j=1}^n \mathcal{I}_{y_i^+ > y_j^-}}{mn} \quad (6)$$

where the numerator corresponds to the Mann-Whitney U-statistic (Mann & Whitney, 1947). The applications that aim directly optimizing the AUC use surrogate convex version of Eq. (6) as a loss function (Gultekin et al., 2020; Gao et al., 2013; Ding et al., 2015; Sulam et al., 2017).

In addition to AUC, True Positive Rate (TPR) and False Positive Rate (FPR) are crucial for characterizing a binary classifier’s behavior at a given operating point. If we assume the classifier outputs a probability for each sample, indicating the probability of belonging to the positive class, the operating point is given by a threshold that is applied to the classifier’s output to perform binary decisions. True Positives are then defined as the positive samples that achieve a higher output than the threshold and False Positives are negative samples for which the classifier’s output surpasses the threshold. TPR/FPR are then defined as the proportion of TP/FP to all positive/negative samples. In this work, we are interested in applications for which the thresholds need to be set such that the final decisions achieve high TPR.

4. Proposed method

Let $F(\theta)$ be a generic loss function that is used to train DNNs. Let us also define $f_{\theta}(x_1^+), \dots, f_{\theta}(x_{N_+}^+)$ and

$f_{\theta}(x_1^-), \dots, f_{\theta}(x_{N_-}^-)$ as the output of a DNN for positive and negative class samples, respectively. We choose the positive class as the minority class in our description, i.e., $N_+ \ll N_-$ and assume that this class is associated with higher risk of making a mistake. We denote the labels of the positive and negative classes as y^+ and y^- , respectively.

We define our constrained optimization problem as follows:

$$\begin{aligned} & \arg \min_{\theta} F(\theta) \\ & \text{subject to } \sum_{k=1}^{N_-} \max\left(0, -(f_{\theta}(x_j^+) - f_{\theta}(x_k^-)) + \delta\right) = 0 \\ & j \in \{1, \dots, N_+\}, \end{aligned} \quad (7)$$

where the constraint states that the output of the DNN for each positive sample should be larger than the outputs of all of the negative samples by a margin δ . Satisfying the constraint would directly ensure maximal AUC.

We define the equivalent unconstrained version of Eq. (7) by writing it in the form given in Eq. (4) using ALM

$$\mathcal{L}_{\mu}(\theta, \lambda) = F(\theta) + \frac{\mu \sum_{j=1}^{N_+} q_j^2}{2 \cdot N_+ \cdot N_-} + \frac{\sum_{j=1}^{N_+} \lambda_j \cdot q_j}{N_+ \cdot N_-} \quad (8)$$

where, $q_j = \sum_{k=1}^{N_-} \max(0, -(f_{\theta}(x_j) - f_{\theta}(x_k)) + \delta)$, μ is the penalty coefficient corresponding to the quadratic penalty term, λ_j is the estimate of Lagrange multiplier corresponding to each positive training sample j , and δ is the margin that we determine using a validation dataset.

Recall that our goal with the constraint and the final augmented loss function is to maximize AUC through minimizing FPR for high TPR. The design of the constraint is crucial to achieve this goal. In Fig. 1, we demonstrate this on a toy example. At the top we show 10 data samples and order them with respect to a classifier’s output for the samples, i.e., samples on the right are assumed to yield higher output than those on the left. The gray area in the figure below shows the AUC for the toy data samples. Consider two different optimizations to increase the AUC. One adds the red box and the other adds the green box to the gray area. Both optimizations lead to exactly the same AUC improvement, however, only adding the green box reduces FPR at the highest TPR.

In the proposed method, we design the constraint to achieve lower FPR at high TPR, such that the optimization can reduce cost more by adding the green box instead of the red box. To see this, let us assume that the distances between all the successive markers in the figure are the same, and we denote this by Δ . Note that the distances between markers indicate the differences between the outputs of the classifiers for the samples corresponding to the markers.

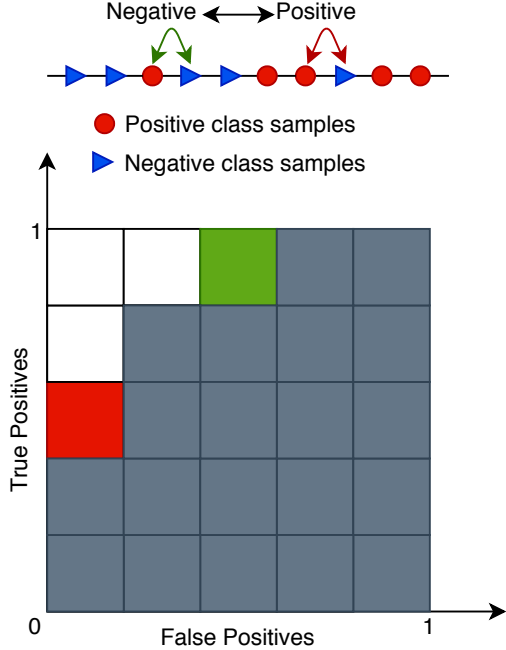


Figure 1. Toy example that illustrates different optimizations that yield the same improvement in AUC. The optimization that adds the green box to the AUC however, leads to lower false positive rate at the highest true positive rate. The augmented Lagrangian given in Eq. (8) prefers adding the green box to improve the AUC rather than the red one.

Let us also further assume that all the Lagrange multipliers have the same value. In this case, one can verify that if the optimization swaps the locations of the left most positive sample (red circle marker) and the negative sample to its immediate right (blue triangle marker), the cost due to the constraint in Eq. (8) will decrease by $39\mu\Delta^2/2 + 3\lambda\Delta$. Swapping the locations of the right most negative sample and the positive sample to its left will decrease the cost due to the constraint by $19\mu\Delta^2/2 + 3\lambda\Delta^2$. So, from the cost perspective, the optimization should prefer the former swap over the latter, which corresponds to adding the green box to the AUC instead of red box. Therefore, the augmented Lagrangian cost would be decreased further when FPR at the highest TPR is reduced rather than increasing the TPR at the lowest FPR. Instead of defining the constraint for each positive sample in Eq. (8), if we were to define it for each negative sample in the exactly opposite way, i.e., $\sum_{j=1}^{N^+} \max(0, -(f_\theta(x_j^+) - f_\theta(x_k^-)) + \delta) = 0$, $k \in \{1, \dots, N^-\}$, then the situation would have been reversed. The optimization would prefer adding the red box over the green box to decrease the cost further. If we were to define a constraint for each positive-negative pair, i.e., $f_\theta(x_j^+) > f_\theta(x_k^-), \forall j$ and k , then adding the red or the

²Derivations for this toy example are provided in Appendix A

green box to improve the AUC would have yielded exactly the same decrease in the cost.

In Algorithm 1, we present the algorithm that we use for estimating the parameters of a DNN, θ , using the proposed loss function in Eq. (8). The parameters θ are updated with every batch using gradient descent with learning rate α . Concurrently, μ is increased using a multiplicative coefficient ρ only when the AUC of validation set (denoted as $ValAUC$ in Algorithm 1) is not improved. We update λ in each iteration for each positive sample.

Algorithm 1 ALM for Training DNNs

Input: $\theta^{(0)}, \mu^{(0)}, \lambda_j^{(0)}, \rho$;
for $t = 1, \dots, T$ **do**
 Get a mini-batch of x_B with size B from training set;
 $y_B = f(X_B)$;
 Calculate $q_j^{(t)}$; $\forall j \in [1, B]$ and $y_j = y^+$
 $\theta^{(t+1)} \leftarrow \theta^{(t)} - \alpha \cdot \nabla_{\theta} \mathcal{L}_{\mu}(\theta^{(t)}, \lambda)$;
 $\lambda_j^{(t+1)} \leftarrow \lambda_j^{(t)} + \mu^{(t)} \cdot q_j^{(t)}$; $\forall j \in [1, B]$ and $y_j = y^+$
 #*ValAUC*: Evaluate AUC on validation set
 if $ValAUC^{(t)} < ValAUC^{(t-1)}$ **then**
 $\mu^{(t+1)} \leftarrow \mu^{(t)} \cdot \rho$;
 else
 $\mu^{(t+1)} \leftarrow \mu^{(t)}$;
 end if
end for
Return $\theta^{(t+1)}$

Direct optimization of Eq. (8) from a random initialization of $\theta^{(0)}$ is not easy for DNNs due to many terms involved into the loss function. To mitigate this problem, we initialize $\theta^{(0)}$ by training the DNNs using only $F(\theta)$. As we mentioned earlier, $F(\theta)$ can be any loss function that is used for training DNNs including the ones that are proposed to handle class imbalance. We present results with different choices of $F(\theta)$ in the experiments.

5. Experiments

In this section, we present our experimental evaluations on image-based binary classification tasks. We perform experiments on two datasets: 1) an in-house MRI medical dataset for prostate cancer, 2) a publicly available computer vision dataset, CIFAR10 (Krizhevsky et al., 2009).

In our experiments, we experiment with 8 different existing loss functions most of which have been designed to handle class imbalance: standard binary cross-entropy (BCE), symmetric margin loss (S-ML) (Liu et al., 2016), symmetric focal loss (S-FL) (Lin et al., 2017), asymmetric margin loss (A-ML) and focal loss (A-FL) (Li et al., 2019), cost-weighted BCE (WBCE) (Zadrozny et al., 2003), class-balanced BCE (CB-BCE) (Cui et al., 2019) and mean squared false error

(MSFE) (Wang et al., 2016). We first train DNNs for binary classification using only the loss functions and then using our method that adds the proposed constraint to the loss function and solves Eq. (8), and we compare the classification performances. In addition, we also compare the proposed method with directly optimizing AUC using the mini-batch AUC (MBAUC) method proposed in (Gultekin et al., 2020).

The proposed method is implemented in PyTorch and we run all experiments on a Nvidia GeForce GTX Titan X GPU with 12GB memory.

5.1. Datasets

Prostate MRI dataset consists of 2 distinct cohorts: 1) a group of 300 multiparametric prostate MRI studies used for training and 2) another group of 100 multiparametric prostate MRI studies used for testing the trained DNNs. There is no overlap between the groups. All MRI scans were performed on Siemens Skyra scanners (Siemens Healthineers, Erlangen, Germany) at a field strength of 3 Tesla using a 60 Ch or 18 Ch phased-array body coil. MRI studies for each patient included 3D T2-weighted axial images and corresponding diffusion-weighted images taken at three b-values (100, 600 and 1000 s/mm^2). Two board-certified radiologists with 10 and 7 years of experience in dedicated prostate imaging independently reviewed all examinations of the training set and test set and scored whether Dynamic Contrast Enhanced (DCE) sequences would have been beneficial for diagnosis. After completion of readings a consensus was reached by the two readers by reviewing all examinations with discrepant decisions. The resulting consensus on the training set was used as reference standard for training of the DNN. The goal of the binary classification here is to identify subjects who do not require additional DCE imaging for accurate diagnosis, so they can be spared from unnecessary injection and cost and duration of the scanning can be reduced.

In our experiments, we randomly split 20% of the training cohort as validation set by keeping the class imbalance consistent across the datasets. In both training and testing cohorts, positive samples represent 30% of all the patients which leads to an inherent 1:2 class ratio. Additionally, we induced a higher class ratio of 1:8, in order to perform evaluations with larger class imbalance. Given the limited size of the dataset, we do not reduce the class ratio further to avoid over-fitting.

CIFAR10 dataset contains 50000 training and 10000 testing images from 10 classes. In our experiments, we randomly selected 2 classes among 10 to pose a binary classification problem. We present additional experiments with different randomly chosen classes in Appendix C. To simulate a condition similar to the medical dataset, we use a

small subset of the training set. We randomly sampled 300 images from the negative class (majority) and varying number of images from the positive class (minority) to obtain different class imbalance ratios of 1:2, 1:9, and 1:19. For testing, we use the whole available test set that consists of 1000 images for the negative class and randomly sampled the test images for the positive class such that the class ratio of the training set is retained in the test set. We also perform experiments on the original test sets without considering the class ratio and present in Appendix D.

5.2. Training details

Network architectures: We use a different convolutional neural network (CNN) architecture for each dataset. For the prostate MRI dataset, we use a 3D CNN that consist of cascaded 3D convolution, 3D max-pooling, and activation functions. We use ReLU activation in the intermediate layers while we use Sigmoid in the final output. For the CIFAR10 dataset, we use the same cascaded architecture by replacing the 3D layers with the 2D ones. Architectural details can be found in Appendix B.

Ensembling for higher reliability: In our target applications of medical imaging, model reliability is very crucial. Dealing with small datasets may lead to dataset-dependent results even with the random splits, which could completely hinder objective evaluation. To weaken this phenomenon, we adopt the following ensembling strategy. Given a dataset and a class ratio, we create 10 random stratified splits of the dataset with 80% and 20% portions and train 10 models independently. The larger portions are used for training and the smaller portions for choosing hyper-parameters, e.g., stopping iteration. During inference, all the models are applied on test samples and predictions are averaged in the logit space before the sigmoid function to yield the final prediction. We apply the ensembling to all the models we experiment with. This practice attenuates data dependency and we observed that the final AUC is improved when compared to the average of AUCs of different models. We present supporting experimental results in Appendix B.

Hyper-parameters selection: Selection of the best hyper-parameters is crucial both to ensure proper and fair evaluation of the methods and to understand the true performance of any model. To achieve this, we performed grid-search to determine the hyper-parameters that yielded the highest AUC on the validation set. The test sets in both experiments were not used for hyper-parameter selection. To reduce computational load, we selected the common hyper-parameters such as the optimizer, learning rate, and the activation functions in the DNNs based on their performance using the BCE loss function and fixed them in all experiments.

Besides the common hyper-parameters, the majority of the existing methods have hyper-parameters that crucially af-

fect their performance. Namely, these hyper-parameters are margin m for S-ML and A-ML, exponent γ for S-FL and A-FL, weight of the cost c for WBCE and β for CB-BCE. We selected best values for these hyper-parameters from respective candidate sets that we created based on the information provided in the original papers for each of them.

In the proposed method, there are 4 parameters to be set: $\mu^{(0)}$, $\lambda^{(0)}$, ρ , and δ . $\mu^{(0)}$, $\lambda^{(0)}$, and ρ are stemming from ALM and we follow the guideline from (Bertsekas, 1999) when setting them. We initialized all the Lagrangian multipliers $\lambda_i^{(0)}$ to 0. We choose $\mu^{(0)}$ from the set $\{0.2, 0.3\}$, as it is suggested to choose a small value in the beginning and increase it iteratively using the equation $\mu^{(k+1)} = \rho \cdot \mu^{(k)}$. We choose ρ from the set $\{2, 3, 4\}$ as $\rho > 1$ is suggested. Moreover, we do not increase ρ beyond 4 to avoid potential dominance of the constraint on $F(\theta)$ since ρ is used to increase μ . Once we find the best combination of μ and ρ based on the AUC on the validation set, we fix them and search for δ from the set $\{1.0, 1.5, 2.0\}$. Please see Appendix E for more details on the hyper-parameters selection and model stability for different hyper-parameter choices.

Once the hyper-parameters for each model is selected, the training is performed and models are applied to the test sets to yield the final results, which is described next.

5.3. Results

The results of the experiments on CIFAR10 and the in-house medical imaging dataset are shown in Tables 2 and 1, respectively. We present AUC and FPR at maximal levels of TPR (or minimal levels of false negative rate (FNR)) on the test sets. In the tables, we indicate improvements introduced by ALM with respect to the original loss function with bold font. The best scores in each category are indicated by underlines. We note that the test set employed for each evaluation presents the same data imbalance as its corresponding training set. Consequently, the sets used for evaluation contain different amount of samples at each class imbalance ratio. Therefore, the experimental results across different class imbalance ratios are not directly comparable with each other in these tables.

From the results presented in Table 2, we draw the following observations. Overall, ALM is able to consistently improve the performance of almost all the loss functions with regard to both AUC and FPRs at maximal TPR levels. Even in those cases when AUC is improved to a moderate extent there is still an improvement in FPRs, in accordance with our goal. Moreover, it is noticeable that the higher the imbalance, which represents a major complexity for the baselines, the higher the benefit of applying ALM. This observation is consistent with the outcomes on the MRI images. At higher degree of imbalance, using ALM generally the performance of the loss function, leading to evident improvements in

the metrics in most cases. Overall, at the lower ratio of class imbalance ALM is able to reduce the FPRs, even when AUC is not subject to an increase. Considering that such classifiers in “critical” applications would be operated at high TPR (or low FNR), reduction in FPR in these settings is the effect we desired from the proposed approach. Lastly, we also observe in the tables that directly optimizing AUC via MBAUC does not provide the same improvements as using the proposed ALM approach.

In our analysis we also investigate the consistency of improvements on AUC via DeLong test (DeLong et al., 1988; Sun & Xu, 2014). It aims to assess the statistical significance of AUC of two different models on the same evaluation set. The results are consistent with our finding, smaller p values are overall obtained on CIFAR10 than on MRI set. The variability on the latter, may be due to a higher complexity inherent to this dataset.

6. Conclusion and future work

In this paper, we pose the training of a DNN for binary classification under class imbalance as a constraint optimization problem and propose a novel constraint that can be used with existing loss function. In particular, we design our constraint to optimize AUC such that it emphasizes reduction of FPR at high TPR, considering that DNN-based binary classifiers would be operated at high TPR regimes for “critical” applications. We transfer the the constrained optimization problem into an unconstrained optimization problem using the augmented Lagrangian approach and optimize the resulting loss function using stochastic gradient descent.

In medical imaging, applications with data imbalance are ubiquitous and cost of making some types of mistakes are more severe than others since these classes most often correspond to clinically critical cases. Moreover, there are usually fewer samples for the critical cases which lead to class imbalance and make things more complicated. Therefore, reducing FPR at high TPR is crucially more important.

We evaluated the proposed method on 2 different datasets by simulating different class ratios. Our results demonstrated that the proposed method can improve the performance of existing loss functions designed for class imbalance and achieve the best results in most of the settings by attaining higher AUC and reducing FPR at minimal FPR.

Constrained optimization has received relatively limited attention for training DNNs and we believe there is a strong potential in exploring this field in future research. One possible extension of the proposed method can be achieved through focusing on multi-class classification problems although it is not trivial since AUC is not well-defined in multi-class setting. Another future research could be extend-

Table 1. Evaluation of results on the in-house MRI dataset. Results are shown for class ratio 1:2 (top) and 1:8 (bottom). For convenience number FPR results are given with respect to number of false negatives (FN) instead of TPR.

TRAINING METHOD		TEST AUC	FPR @ 0 FN	FPR @ 1 FN
BCE		92.75	61.5	54.0
S-ML		93.27	54.9	51.6
S-FL		93.62	55.0	42.4
A-ML		93.58	53.4	50.7
A-FL		94.36	38.9	27.7
W-BCE		92.97	54.7	40.6
CB-BCE		93.95	45.3	29.7
MSFE		<u>94.60</u>	43.8	<u>26.6</u>
MBAUC		93.02	75.0	29.7
<hr/>				
ALM WITH	BCE	92.96	50.0	34.4
	S-ML	92.23	54.7	31.3
	S-FL	92.38	45.3	29.7
	A-ML	92.87	46.8	45.4
	A-FL	94.29	37.0	31.3
	W-BCE	92.29	54.0	40.0
	CB-BCE	94.14	42.2	37.5
	MSFE	93.75	48.4	32.8
<hr/>				
BCE		88.09	40.6	36.6
S-ML		88.86	46.9	23.4
S-FL		86.71	35.9	26.6
A-ML		91.20	35.9	28.1
A-FL		83.60	100.0	25.0
W-BCE		89.45	31.3	23.4
CB-BCE		85.94	48.4	31.3
MSFE		90.82	23.4	20.3
MBAUC		88.28	28.1	25.0
<hr/>				
ALM WITH	BCE	92.96	21.8	12.5
	S-ML	93.95	20.3	9.4
	S-FL	89.84	28.1	21.9
	A-ML	96.88	10.9	7.8
	A-FL	86.72	64.1	29.7
	W-BCE	88.7	26.2	18.8
	CB-BCE	88.09	37.5	26.6
	MSFE	90.43	25.0	20.3

ing our method to binary segmentation tasks which have an inherent class imbalance problem since most of the pixels belong to background in many applications like medical imaging.

Table 2. Evaluation of results on CIFAR10 dataset. From top to bottom, results are shown for class ratio 1:2, 1:9, 1:19.

TRAINING METHOD		TEST AUC	FPR @ 100% TPR	FPR @ 95% TPR	FPR @ 90% TPR
BCE		94.67	69.1	20.9	15.2
S-ML		94.57	68.2	21.6	15.2
S-FL		94.74	64.3	22.0	15.6
A-ML		94.56	67.0	21.8	15.6
A-FL		94.87	65.1	20.1	13.8
W-BCE		94.54	68.7	21.9	15.6
CB-BCE		94.38	69.3	23.5	16.3
MSFE		93.84	70.2	23.3	17.1
MBAUC		94.26	69.6	23.80	15.40
<hr/>					
ALM WITH	BCE	95.41	66.2	21.1	13.2
	S-ML	95.10	61.9	21.9	13.5
	S-FL	95.22	54.3	20.5	14.7
	A-ML	95.18	65.0	21.4	14.3
	A-FL	94.95	64.0	20.5	14.7
	W-BCE	95.67	59.9	18.7	13.2
	CB-BCE	95.47	58.8	18.5	13.4
	MSFE	95.27	69.9	19.9	13.2
<hr/>					
BCE		93.96	41.3	20.6	16.6
S-ML		94.04	39.6	20.3	16.2
S-FL		93.39	39.7	19.4	17.6
A-ML		93.64	42.1	21.3	17.3
A-FL		93.70	42.0	20.9	17.1
W-BCE		91.12	54.1	30.5	23.4
CB-BCE		90.83	58.5	31.7	27.1
MSFE		91.24	52.0	32.6	19.9
MBAUC		92.04	44.1	22.7	17.0
<hr/>					
ALM WITH	BCE	94.74	34.2	19.9	14.1
	S-ML	94.98	28.5	20.0	14.0
	S-FL	94.2	35.6	22.5	17.4
	A-ML	94.87	32.9	18.9	13.6
	A-FL	95.38	31.4	16.5	12.4
	W-BCE	93.03	47.9	23.1	19.8
	CB-BCE	93.89	38.5	22.7	17.9
	MSFE	93.83	39.3	22.2	14.9
<hr/>					
BCE		91.95	40.4	27.9	21.1
S-ML		92.28	36.4	27.9	22.0
S-FL		92.17	39.3	<u>23.5</u>	22.7
A-ML		91.74	34.2	<u>27.4</u>	22.6
A-FL		91.88	45.8	32.5	21.7
W-BCE		88.85	61.2	41.2	32.7
CB-BCE		88.24	61.6	36.5	35.1
MSFE		88.37	59.7	38.0	35.0
MBAUC		91.8	36.00	26.4	25.0
<hr/>					
ALM WITH	BCE	93.21	29.8	27.5	17.2
	S-ML	93.76	28.4	24.1	17.9
	S-FL	93.50	31.0	<u>23.5</u>	16.8
	A-ML	93.06	29.0	26.2	22.4
	A-FL	93.45	34.4	27.7	22.3
	W-BCE	91.22	48.2	31.2	19.6
	CB-BCE	90.80	52.6	42.1	25.7
	MSFE	91.02	49.9	32.5	22.9

A. Additional example to compare the proposed constraint with the alternative one

In this section, we present an additional visual example that shows that the proposed constraint focuses more on correcting positive (minority) class samples than the alternative version (described in the visual example in Sec. 4 of the main paper). Below derivations are given for generic number of positive and negative examples. The additional loss equations given for the visual example in the main paper can be derived similarly.

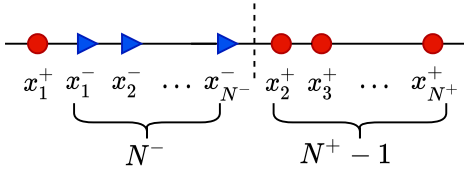


Figure 2. Illustrative example

Let us assume that we are given N^+ positive and N^- negative class samples as shown in Fig. 2.

Using the loss with the proposed constraint λ is updated as follows:

$$\lambda = \lambda_{x_1^+} + \mu \sum_{k=1}^{N^-} -f(x_1^+) + f(x_k^-)$$

Then, the loss with the proposed constraint is written as follows:

$$L_\mu(\theta, \lambda) = F(\theta) + \mu \left(\sum_{k=1}^{N^-} -f(x_1^+) + f(x_k^-) \right)^2 + \left(\lambda + \mu \sum_{k=1}^{N^-} -f(x_1^+) + f(x_k^-) \right) \left(\sum_{k=1}^{N^-} -f(x_1^+) + f(x_k^-) \right) \quad (9)$$

We can further simplify the above equation by assuming that the distances between the consecutive data samples are equal and denoted by Δ :

$$L_\mu(\theta, \lambda) = F(\theta) + \mu (\Delta + 2\Delta + \dots + N^- \Delta)^2 + \lambda (\Delta + 2\Delta + \dots + N^- \Delta) + \mu (\Delta + 2\Delta + \dots + N^- \Delta)^2 \quad (10)$$

which can be further simplified as

$$L_\mu(\theta, \lambda) = F(\theta) + 2\mu\Delta^2 \left(\frac{N^-(N^- + 1)}{2} \right)^2 + \lambda\Delta \left(\frac{N^-(N^- + 1)}{2} \right) \quad (11)$$

Using the loss with the alternative constraint, there are λ for each negative samples and let us denote all of them with the same notation for simplicity:

$$\lambda = \lambda_{x_1^-} + \mu(-f(x_1^+) + f(x_1^-))$$

⋮

$$\lambda = \lambda_{x_{N^-}^-} + \mu(-f(x_1^+) + f(x_{N^-}^-))$$

Then, the loss with the alternative constraint, L^* , is as follows:

$$L_\mu^*(\theta, \lambda) = F(\theta) + \mu \sum_{k=1}^{N^-} \left(-f(x_1^+) + f(x_k^-) \right)^2 + \sum_{k=1}^{N^-} \left(\lambda + \mu(-f(x_1^+) + f(x_k^-)) \right) \left(-f(x_1^+) + f(x_k^-) \right) \quad (12)$$

We can further simplify the above equation by assuming that the distances between the consecutive data samples are equal and denoted by Δ :

$$L_\mu^*(\theta, \lambda) = F(\theta) + 2\mu\Delta^2 \left(\frac{N^-(N^- + 1)(2N^- + 1)}{6} \right) + \lambda\Delta \left(\frac{N^-(N^- + 1)}{2} \right) \quad (13)$$

From Eq. (11) and (13), we can observe that the proposed loss assigns more penalty due to the misclassification of the positive samples compared to the alternative penalty.

B. Additional training details

We employ two DNN architectures, one for each dataset, given the inherent differences between them. In particular, for the MRI dataset, the network is composed by two, identical and parallel structures. For each patient, one path of the NN processes the diffusion-weighted images and the other part processes the T2-weighted axial images. Each path consists of cascaded 3D convolution, 3D max-pooling, and activation functions. Finally, in the fully connected layer the

outputs are concatenated, as the different modalities bring complementary information. For CIFAR10 we use a single-path, 2D architecture, whose layers are the same as for MRI, substituting 3D with 2D versions.

In our experiments, we create 10 random stratified splits of the dataset and train 10 models independently for each dataset and class ratio. In test time, all the models are applied on test samples and logits of the predictions (before the sigmoid function) are averaged to yield the final prediction. To demonstrate the effectiveness of this ensembling strategy, we compare the results obtained with ensembling against the performance of the individual 10 models. The results in Tables 3 and 4 show that average AUC of these 10 models are less than the AUC results obtained by the ensembling approach for the MRI and CIFAR10 datasets, respectively.

For the MRI dataset which is inherently a small dataset, we randomly shuffled the whole dataset before creating each 80-20% split. To create each split for majority class in CIFAR10, we randomly selected 300 samples for training and 100 for validation from class 0. For the minority class, we randomly selected sufficient amount of samples from class 1 of CIFAR10 to obtain the desired class ratio. Given the larger amount of data in the original CIFAR10, we opt to randomly sample the training and validation set from the whole set to demonstrate that our model does not depend on partitioning the dataset. An alternative of sampling a small subset once and creating splits from it emphasizes partitioning independence less strongly.

C. Additional experiments on CIFAR10 dataset

In the main paper, we presented the results for CIFAR10 by arbitrarily selecting 2 classes: class 0 and class 1. In order to demonstrate that the results are consistent across different choices, we performed further experiments by arbitrarily selecting another 2 classes: class 6 (majority) and class 7 (minority). We carried out this experiments in an exactly similar way as we do the previous CIFAR10 experiments in terms of constructing the training/validation splits, hyperparameter search and so on. We present the results of this additional experiments in Table 5. The results show that ALM is able to steadily improve the performance of the other methods in almost all cases in terms of both AUC and FPRs at maximal TPR levels which are consistent with the experiments in the main paper.

D. Experiments on the whole test sets on CIFAR10

In the CIFAR10 experiments, we constructed the test sets to retain the class imbalance ratios in the training sets since

Table 3. Improvement achieved by the ensembling approach compared to the individual performance of 10 models for MRI dataset. From top to bottom, results are shown for class ratio 1:2, 1:8.

Training method	Ensembling AUC	Average AUC	
BCE	92.75	89.1 ± 5.0	
S-ML	93.27	88.56 ± 5.5	
S-FL	93.62	88.21 ± 4.9	
A-ML	93.58	88.28 ± 5.3	
A-FL	94.36	89.2 ± 5.0	
W-BCE	92.97	88.08 ± 5.7	
CB-BCE	93.95	88.91 ± 5.2	
MSFE	94.60	89.9 ± 6.3	
MBAUC	93.02	83.5 ± 8.4	
ALM with	BCE	92.96	87.95 ± 3.7
	S-ML	92.23	88.47 ± 3.0
	S-FL	92.38	87.86 ± 2.4
	A-ML	92.87	88.77 ± 3.6
	A-FL	94.29	88.01 ± 4.6
	W-BCE	92.29	87.56 ± 4.3
	CB-BCE	94.14	87.97 ± 4.9
	MSFE	93.75	88.45 ± 5.1
BCE	88.09	79.82 ± 7.5	
S-ML	88.86	80.31 ± 7.3	
S-FL	86.71	77.05 ± 9.9	
A-ML	91.20	81.44 ± 8.3	
A-FL	83.60	78.88 ± 9.4	
W-BCE	89.45	78.36 ± 9.3	
CB-BCE	85.94	78.98 ± 9.8	
MSFE	90.82	79.22 ± 9.1	
MBAUC	88.28	73.36 ± 12.3	
ALM with	BCE	92.96	78.69 ± 9.4
	S-ML	93.95	79.59 ± 11.3
	S-FL	89.84	79.31 ± 7.6
	A-ML	96.88	79.51 ± 8.7
	A-FL	86.72	77.89 ± 6.44
	W-BCE	88.70	75.89 ± 10.2
	CB-BCE	88.09	78.69 ± 9.6
	MSFE	90.43	80.05 ± 8.9

this is a more realistic scenario for a real use case of the methods to handle class imbalance. Additionally, we present the results by using the original test images in Table 6. Note that using the full balanced test set leads to degradation in the results compared to using test sets that retains the class imbalance ratio. Additionally, as the class imbalance ratio increases, the accuracy drops more drastically in the balanced test sets compared to the imbalanced ones presented in the main paper. This can be explained by the fact that the balanced test data distribution is different than the training data distributions.

E. Best parameters combinations

In Tables 7 and 8, we present the best hyperparameter combinations based on the validation sets for the experiments in

the main paper.

We searched the hyperparameter space incrementally in order to slightly reduce the number of simulations we run for computational purposes. Common hyperparameters such as number of epochs, learning rate, batch size and patience for early stopping have been selected based on the best validation AUC of BCE for each dataset with class ratio 1:2. Then, these parameters are kept fixed for all the experiments. Next, for the baselines having specific hyperparameters the search has been carried out specifically for each dataset as well as for each class ratio, among those values proposed by the original papers (apart from WBCE for which does not provide specific guideline for setting the weight of the loss, thus we decided to set it proportionate to the class ratio N for minority class samples). More specifically, for the baselines the search has been done among the following values:

- margin m has been searched among $\{0.1, 0.5, 2, 4\}$ for s-ML and a-ML
- exponent γ has been searched among $\{1, 2, 4, 5\}$ for s-FL and a-FL
- weight coefficient m has been searched among $\{N/3, 2N/3, N\}$ for WBCE, being N the class ratio
- exponent β has been searched among $\{0.99, 0.999, 0.9999\}$ for cb-BCE

Once the hyperparameters of the baselines are set, we kept them fixed for ALM training. We kept searching for the hyperparameters of ALM. With the same logic, we perform a grid search with varying ρ and μ^0 . We choose $\mu^{(0)}$ from the set $\{0.2, 0.3\}$ and ρ from the set $\{2, 3, 4\}$. Once we find the best combination of μ and ρ based on the AUC on the validation set, we fix them and search for δ from the set $\{1.0, 1.5, 2.0\}$. We discarded the combination $(\mu^{(0)}, \rho) = (0.2, 2)$ as we observed it is not effective in our set-up from preliminary analysis.

Table 4. Improvement achieved by the ensembling approach compared to the individual performance of 10 models for CIFAR10 dataset. From top to bottom, results are shown for class ratio 1:2, 1:9, 1:19.

TRAINING METHOD		ENSEMBLING AUC	AVERAGE AUC
	BCE	94.67	91.67 \pm 0.9
	S-ML	94.57	91.60 \pm 0.9
	S-FL	94.74	91.4 \pm 1.0
	A-ML	94.56	91.65 \pm 1.0
	A-FL	94.87	91.83 \pm 0.6
	W-BCE	94.54	92.05 \pm 0.8
	CB-BCE	94.38	91.97 \pm 0.7
	MSFE	93.84	91.9 \pm 0.4
	MBAUC	94.26	91.57 \pm 0.7
ALM WITH	BCE	95.41	92.09 \pm 1.1
	S-ML	95.10	91.88 \pm 1.1
	S-FL	95.22	91.97 \pm 1.0
	A-ML	95.18	91.9 \pm 1.1
	A-FL	94.95	91.95 \pm 0.5
	W-BCE	95.67	92.42 \pm 0.9
	CB-BCE	95.47	92.12 \pm 0.9
	MSFE	95.27	92.42 \pm 0.8
	BCE	93.96	88.86 \pm 2.7
	S-ML	94.04	89.1 \pm 2.6
	S-FL	93.39	88.31 \pm 1.0
	A-ML	93.64	88.74 \pm 2.7
	A-FL	93.70	88.58 \pm 2.5
	W-BCE	91.12	86.96 \pm 2.8
	CB-BCE	90.83	86.79 \pm 2.8
	MSFE	91.24	87.32 \pm 2.3
	MBAUC	92.04	88.22 \pm 2.2
ALM WITH	BCE	94.74	89.47 \pm 2.4
	S-ML	94.98	89.64 \pm 2.5
	S-FL	94.2	88.0 \pm 3.5
	A-ML	94.87	89.18 \pm 2.5
	A-FL	95.38	89.12 \pm 3.4
	W-BCE	93.03	87.48 \pm 2.6
	CB-BCE	93.89	88.33 \pm 2.0
	MSFE	93.83	88.20 \pm 2.6
	BCE	91.95	86.51 \pm 3.7
	S-ML	92.28	85.76 \pm 3.8
	S-FL	92.17	87.73 \pm 2.7
	A-ML	91.74	83.92 \pm 5.6
	A-FL	91.88	87.05 \pm 3.2
	W-BCE	88.85	85.13 \pm 4.2
	CB-BCE	88.24	80.19 \pm 7.2
	MSFE	88.37	83.69 \pm 5.7
	MBAUC	91.8	86.03 \pm 3.6
ALM WITH	BCE	93.21	88.55 \pm 3.2
	S-ML	93.76	87.13 \pm 3.6
	S-FL	93.50	86.59 \pm 4.5
	A-ML	93.06	86.29 \pm 4.4
	A-FL	93.45	86.49 \pm 4.0
	W-BCE	91.22	85.06 \pm 3.6
	CB-BCE	90.80	83.11 \pm 7.0
	MSFE	91.02	84.14 \pm 5.8

Table 5. Results of the additional experiments on CIFAR10 dataset with two different and arbitrarily chosen classes (class 6 and 7). From top to bottom, results are shown for class ratio 1:2, 1:9, 1:19.

TRAINING METHOD	TEST AUC	FPR @ 100% TPR	FPR @ 95% TPR	FPR @ 90% TPR	
BCE	95.38	79.6	22.2	13.4	
S-ML	95.47	78.4	22.9	12.8	
S-FL	95.77	77.3	21.0	11.2	
A-ML	95.50	78.8	22.0	13.4	
A-FL	95.65	82.3	21.9	11.6	
W-BCE	95.54	74.4	21.4	12.4	
CB-BCE	95.54	75.7	21.6	12.7	
MSFE	95.3	71.6	23.9	15.2	
MBAUC	95.37	75.0	23.2	12.6	
<hr/>					
ALM WITH	BCE	96.03	73.3	17.4	10.9
	S-ML	96.27	71.9	16.4	9.9
	S-FL	96.65	72.5	16.0	8.5
	A-ML	96.38	73.2	17.0	9.9
	A-FL	96.45	71.7	16.4	9.4
	W-BCE	96.26	69.8	18.6	9.9
	CB-BCE	96.47	68.9	16.1	10.8
MSFE	96.53	66.7	16.7	9.9	
<hr/>					
BCE	95.21	55.5	23.6	14.5	
S-ML	95.11	56.0	23.3	14.9	
S-FL	95.32	50.3	28.0	12.8	
A-ML	95.22	54.0	21.8	14.8	
A-FL	95.36	56.6	26.2	13.3	
W-BCE	94.87	46.9	26.3	16.6	
CB-BCE	95.1	47.6	24.2	14.5	
MSFE	94.05	46.8	31.8	18.4	
MBAUC	94.16	44.5	30.0	22.6	
<hr/>					
ALM WITH	BCE	96.23	47.0	18.5	12.2
	S-ML	95.47	46.4	19.3	12.8
	S-FL	95.75	49.0	23.5	12.0
	A-ML	96.11	42.0	20.7	11.0
	A-FL	96.13	40.4	18.5	10.0
	W-BCE	94.7	41.4	25.5	20.6
	CB-BCE	95.22	40.7	23.4	18.2
MSFE	95.86	41.4	23.4	13.0	
<hr/>					
BCE	91.64	59.7	32.0	26.5	
S-ML	91.71	57.1	31.45	26.0	
S-FL	91.49	69.0	33.5	30.1	
A-ML	92.54	42.7	30.8	23.3	
A-FL	91.4	68.9	36.7	26.4	
W-BCE	87.89	61.5	35.8	28.3	
CB-BCE	86.14	58.8	52.2	40.9	
MSFE	85.26	64.2	50.0	43.5	
MBAUC	89.85	42.7	32.9	23.2	
<hr/>					
ALM WITH	BCE	93.41	51.5	28.0	20.8
	S-ML	93.19	38.7	31.4	22.0
	S-FL	93.53	48.9	26.65	22.4
	A-ML	92.83	57.5	32.95	19.1
	A-FL	92.9	50.6	32.9	20.5
	W-BCE	88.8	62.2	36.3	32.3
	CB-BCE	89.2	64.6	39.2	33.7
MSFE	89.32	51.3	40.4	31.4	

Table 6. Quantitative results obtained by evaluation the CIFAR10 models in the main paper on the balanced test sets instead of the imbalanced ones. From top to bottom, results are shown for class ratio 1:2, 1:9, 1:19.

TRAINING METHOD	TEST AUC	FPR @ 100% TPR	FPR @ 95% TPR	FPR @ 90% TPR	
BCE	94.82	69.1	20.9	13.4	
S-ML	94.74	68.2	21.2	13.7	
S-FL	94.98	64.3	20.1	14.8	
A-ML	94.73	67.0	21.6	14.8	
A-FL	95.06	65.1	20.1	12.7	
W-BCE	94.71	68.7	20.6	13.8	
CB-BCE	94.56	69.3	21.7	14.2	
MSFE	94.03	70.2	22.8	15.9	
MBAUC	93.66	67.5	23.3	25.6	
<hr/>					
ALM WITH	BCE	95.53	66.2	20.0	12.6
	S-ML	95.28	61.9	20.4	13.2
	S-FL	95.37	60.0	19.3	13.0
	A-ML	95.24	65.0	21.1	13.5
	A-FL	95.18	64.0	19.4	13.2
	W-BCE	95.75	59.9	18.3	12.6
	CB-BCE	95.59	58.8	18.3	13.2
MSFE	95.39	69.9	19.1	13.0	
<hr/>					
BCE	92.36	79.0	29.1	20.8	
S-ML	92.46	79.8	28.9	20.5	
S-FL	91.9	80.7	30.2	20.9	
A-ML	92.12	79.0	29.5	20.7	
A-FL	92.30	78.2	28.7	20.9	
W-BCE	89.85	89.9	36.9	26.9	
CB-BCE	89.60	90.5	38.2	27.4	
MSFE	89.88	77.0	36.0	26.2	
MBAUC	90.97	74.3	32.3	21.3	
<hr/>					
ALM WITH	BCE	93.03	82.5	28.5	18.6
	S-ML	93.11	86.11	28.2	18.9
	S-FL	92.57	83.2	28.5	20.1
	A-ML	93.22	83.4	27.6	18.5
	A-FL	93.51	86.4	26.8	17.3
	W-BCE	91.64	76.4	30.8	21.5
	CB-BCE	92.16	81.7	30.4	20.7
MSFE	92.28	86.2	28.5	20.0	
<hr/>					
BCE	89.47	82.3	38.9	28.9	
S-ML	90.2	78.6	37.7	26.6	
S-FL	89.71	83.2	29.1	27.1	
A-ML	90.3	79.8	35.6	26.2	
A-FL	89.63	85.7	38.2	27.8	
W-BCE	87.79	91.1	44.9	34.4	
CB-BCE	86.76	92.8	47.7	35.4	
MSFE	86.62	92.8	49.1	36.4	
MBAUC	88.38	82.7	39.9	29.2	
<hr/>					
ALM WITH	BCE	90.9	74.7	32.8	25.7
	S-ML	91.45	79.5	32.5	22.5
	S-FL	91.19	79.2	33.3	25.5
	A-ML	91.18	80.9	33.8	23.5
	A-FL	91.04	79.1	34.4	25.0
	W-BCE	89.29	85.3	40.0	28.9
	CB-BCE	89.11	87.0	40.0	30.0
MSFE	89.09	90.2	40.2	29.7	

Table 7. Best hyperparameters based on validation AUC for the in-house MRI dataset. Results are shown for class ratio 1:2 (top) and 1:8 (bottom).

Training method	Best Parameters
BCE	-
S-ML	$m = 0.1$
S-FL	$g = 1.0$
A-ML	$m = 0.1$
A-FL	$g = 2.0$
W-BCE	$c = N/3$
CB-BCE	$\beta = 0.99$
MSFE	-
MBAUC	-

ALM with	BCE	$\mu = 0.3, \rho = 3, \delta = 1.0$
	S-ML	$\mu = 0.3, \rho = 2, \delta = 1.0$
	S-FL	$\mu = 0.3, \rho = 3, \delta = 1.0$
	A-ML	$\mu = 0.2, \rho = 3, \delta = 1.5$
	A-FL	$\mu = 0.3, \rho = 3, \delta = 1.5$
	W-BCE	$\mu = 0.2, \rho = 3, \delta = 2.0$
	CB-BCE	$\mu = 0.3, \rho = 2, \delta = 1.5$
	MSFE	$\mu = 0.2, \rho = 4, \delta = 1.0$

BCE	-
S-ML	$m = 0.1$
S-FL	$g = 2.0$
A-ML	$m = 2.0$
A-FL	$g = 4.0$
W-BCE	$c = N/3$
CB-BCE	$\beta = 0.99$
MSFE	-
MBAUC	-

ALM with	BCE	$\mu = 0.2, \rho = 4, \delta = 2.0$
	S-ML	$\mu = 0.2, \rho = 3, \delta = 1.0$
	S-FL	$\mu = 0.2, \rho = 3, \delta = 1.0$
	A-ML	$\mu = 0.2, \rho = 3, \delta = 1.0$
	A-FL	$\mu = 0.3, \rho = 3, \delta = 1.0$
	W-BCE	$\mu = 0.3, \rho = 2, \delta = 1.5$
	CB-BCE	$\mu = 0.2, \rho = 3, \delta = 1.0$
	MSFE	$\mu = 0.3, \rho = 4, \delta = 1.0$

Table 8. Best hyperparameters based on validation AUC for the CIFAR10 dataset. From top to bottom, results are shown for class ratio 1:2, 1:9, 1:19.

Training method	Best Parameters
BCE	-
S-ML	$m = 0.1$
S-FL	$g = 5.0$
A-ML	$m = 0.5$
A-FL	$g = 4.0$
W-BCE	$c = N/3$
CB-BCE	$\beta = 0.99$
MSFE	-
MBAUC	-

ALM with	BCE	$\mu = 0.2, \rho = 4, \delta = 2.0$
	S-ML	$\mu = 0.3, \rho = 2, \delta = 1.5$
	S-FL	$\mu = 0.3, \rho = 3, \delta = 1.5$
	A-ML	$\mu = 0.2, \rho = 4, \delta = 1.0$
	A-FL	$\mu = 0.3, \rho = 2, \delta = 1.0$
	W-BCE	$\mu = 0.3, \rho = 4, \delta = 1.0$
	CB-BCE	$\mu = 0.3, \rho = 2, \delta = 1.0$
	MSFE	$\mu = 0.3, \rho = 3, \delta = 1.0$

BCE	-
S-ML	$m = 0.1$
S-FL	$g = 4.0$
A-ML	$m = 0.5$
A-FL	$g = 2.0$
W-BCE	$c = N$
CB-BCE	$\beta = 0.9999$
MSFE	-
MBAUC	-

ALM with	BCE	$\mu = 0.2, \rho = 4, \delta = 1.0$
	S-ML	$\mu = 0.3, \rho = 4, \delta = 1.0$
	S-FL	$\mu = 0.3, \rho = 4, \delta = 2.0$
	A-ML	$\mu = 0.3, \rho = 4, \delta = 2.0$
	A-FL	$\mu = 0.3, \rho = 3, \delta = 2.0$
	W-BCE	$\mu = 0.2, \rho = 3, \delta = 1.0$
	CB-BCE	$\mu = 0.2, \rho = 4, \delta = 2.0$
	MSFE	$\mu = 0.3, \rho = 3, \delta = 2.0$

BCE	-
S-ML	$m = 0.1$
S-FL	$g = 2.0$
A-ML	$m = 4.0$
A-FL	$g = 2.0$
W-BCE	$c = N/3$
CB-BCE	$\beta = 0.999$
MSFE	-
MBAUC	-

ALM with	BCE	$\mu = 0.3, \rho = 4, \delta = 1.0$
	S-ML	$\mu = 0.2, \rho = 4, \delta = 1.5$
	S-FL	$\mu = 0.3, \rho = 4, \delta = 2.0$
	A-ML	$\mu = 0.3, \rho = 2, \delta = 2.0$
	A-FL	$\mu = 0.3, \rho = 2, \delta = 2.0$
	W-BCE	$\mu = 0.2, \rho = 3, \delta = 1.0$
	CB-BCE	$\mu = 0.2, \rho = 3, \delta = 1.0$
	MSFE	$\mu = 0.2, \rho = 3, \delta = 1.5$

References

- Bertsekas, D. *Nonlinear Programming*. Athena Scientific, 1999.
- Bertsekas, D. P. Multiplier methods: A survey. *Automatica*, 12(2):133 – 145, 1976. ISSN 0005-1098. doi: [https://doi.org/10.1016/0005-1098\(76\)90077-7](https://doi.org/10.1016/0005-1098(76)90077-7). URL <http://www.sciencedirect.com/science/article/pii/0005109876900777>.
- Buda, M., Maki, A., and Mazurowski, M. A. A systematic study of the class imbalance problem in convolutional neural networks. *Neural Networks*, 106:249 – 259, 2018. ISSN 0893-6080. doi: <https://doi.org/10.1016/j.neunet.2018.07.011>. URL <http://www.sciencedirect.com/science/article/pii/S0893608018302107>.
- Chan, R., Rottmann, M., Hüger, F., Schlicht, P., and Gottschalk, H. Application of decision rules for handling class imbalance in semantic segmentation. *arXiv preprint arXiv:1901.08394*, 2019.
- Chawla, N. V., Bowyer, K. W., Hall, L. O., and Kegelmeyer, W. P. Smote: Synthetic minority over-sampling technique. *J. Artif. Int. Res.*, 16(1):321–357, June 2002. ISSN 1076-9757.
- Cortes, C. and Mohri, M. Auc optimization vs. error rate minimization. *Advances in neural information processing systems*, 16(16):313–320, 2004.
- Cui, Y., Jia, M., Lin, T.-Y., Song, Y., and Belongie, S. Class-balanced loss based on effective number of samples. In *Proceedings of the IEEE/CVF Conference on Computer Vision and Pattern Recognition*, pp. 9268–9277, 2019.
- DeLong, E., DeLong, D., and Clarke-Pearson, D. Comparing the areas under two or more correlated receiver operating characteristic curves: a nonparametric approach. *Biometrics*, 44(3):837–845, September 1988. ISSN 0006-341X. doi: 10.2307/2531595.
- Ding, Y., Zhao, P., Hoi, S. C. H., and Ong, Y.-S. An adaptive gradient method for online auc maximization. *AAAI’15*, pp. 2568–2574. AAAI Press, 2015. ISBN 0262511290.
- Djavan, B., Zlotta, A., Remzi, M., Ghawidel, K., Basharkhah, A., Schulman, C., and Marberger, M. Optimal predictors of prostate cancer on repeat prostate biopsy: a prospective study of 1,051 men. *The Journal of urology*, 163 4:1144–8; discussion 1148–9, 2000.
- Drummond, C., Holte, R. C., et al. C4. 5, class imbalance, and cost sensitivity: why under-sampling beats over-sampling. In *Workshop on learning from imbalanced datasets II*, volume 11, pp. 1–8. Citeseer, 2003.
- Gao, W., Jin, R., Zhu, S., and Zhou, Z.-H. One-pass auc optimization. In *International conference on machine learning*, pp. 906–914. PMLR, 2013.
- Gultekin, S., Saha, A., Ratnaparkhi, A., and Paisley, J. Mba: mini-batch auc optimization. *IEEE transactions on neural networks and learning systems*, 31(12):5561–5574, 2020.
- Haibo He, Yang Bai, Garcia, E. A., and Shutao Li. Adasyn: Adaptive synthetic sampling approach for imbalanced learning. In *2008 IEEE International Joint Conference on Neural Networks (IEEE World Congress on Computational Intelligence)*, pp. 1322–1328, 2008. doi: 10.1109/IJCNN.2008.4633969.
- Hanley, J. and Mcneil, B. The meaning and use of the area under a receiver operating characteristic (roc) curve. *Radiology*, 143:29–36, 05 1982. doi: 10.1148/radiology.143.1.7063747.
- He, H. and Garcia, E. Learning from imbalanced data. *Knowledge and Data Engineering, IEEE Transactions on*, 21:1263 – 1284, 10 2009. doi: 10.1109/TKDE.2008.239.
- Hestenes, M. R. Multiplier and gradient methods. *Journal of optimization theory and applications*, 4(5):303–320, 1969.
- Huang, C., Li, Y., Loy, C. C., and Tang, X. Learning deep representation for imbalanced classification. In *Proceedings of the IEEE conference on computer vision and pattern recognition*, pp. 5375–5384, 2016.
- Krizhevsky, A., Hinton, G., et al. Learning multiple layers of features from tiny images. 2009.
- Lawrence, S., Burns, I., Back, A., Tsoi, A., and Giles, C. L. Neural network classification and prior class probabilities. In *Neural Networks: Tricks of the Trade*, 1996.
- Li, Z., Kamnitsas, K., and Glocker, B. Overfitting of neural nets under class imbalance: Analysis and improvements for segmentation. In *International Conference on Medical Image Computing and Computer-Assisted Intervention*, pp. 402–410. Springer, 2019.
- Lin, T.-Y., Goyal, P., Girshick, R., He, K., and Dollár, P. Focal loss for dense object detection. In *Proceedings of the IEEE international conference on computer vision*, pp. 2980–2988, 2017.
- Litjens, G., Kooi, T., Bejnordi, B. E., Setio, A. A. A., Ciompi, F., Ghafoorian, M., van der Laak, J. A., van Ginneken, B., and Sánchez, C. I. A survey on deep learning in medical image analysis. *Medical Image Analysis*, 42:60–88, Dec 2017. ISSN 1361-8415. doi: 10.1016/j.media.2017.07.005. URL <http://dx.doi.org/10.1016/j.media.2017.07.005>.

-
- Liu, W., Wen, Y., Yu, Z., and Yang, M. Large-margin softmax loss for convolutional neural networks. In *ICML*, volume 2, pp. 7, 2016.
- Liu, Z., Wei, P., Jiang, J., Cao, W., Bian, J., and Chang, Y. Mesa: Boost ensemble imbalanced learning with meta-sampler. In *Conference on Neural Information Processing Systems*, 2020.
- Mann, H. B. and Whitney, D. R. On a test of whether one of two random variables is stochastically larger than the other. *The annals of mathematical statistics*, pp. 50–60, 1947.
- Nocedal, J. and Wright, S. J. *Numerical Optimization*. Springer, New York, NY, USA, second edition, 2006.
- Rakotomamonjy, A. Optimizing area under roc curve with svms. In *ROCAI*, pp. 71–80, 2004.
- Shamsolmoali, P., Zareapoor, M., Shen, L., Sadka, A. H., and Yang, J. Imbalanced data learning by minority class augmentation using capsule adversarial networks. *Neuro-computing*, 2020.
- Sulam, J., Ben-Ari, R., and Kisilev, P. Maximizing auc with deep learning for classification of imbalanced mammogram datasets. In *VCBM*, pp. 131–135, 2017.
- Sun, X. and Xu, W. Fast implementation of delong’s algorithm for comparing the areas under correlated receiver operating characteristic curves. *IEEE Signal Processing Letters*, 21(11):1389–1393, 2014. doi: 10.1109/LSP.2014.2337313.
- Thai-Nghe, N., Gantner, Z., and Schmidt-Thieme, L. Cost-sensitive learning methods for imbalanced data. In *The 2010 International joint conference on neural networks (IJCNN)*, pp. 1–8. IEEE, 2010.
- Tian, J., Liu, Y.-C., Glaser, N., Hsu, Y.-C., and Kira, Z. Posterior re-calibration for imbalanced datasets, 2020.
- Wang, S., Liu, W., Wu, J., Cao, L., Meng, Q., and Kennedy, P. J. Training deep neural networks on imbalanced data sets. In *2016 international joint conference on neural networks (IJCNN)*, pp. 4368–4374. IEEE, 2016.
- Ying, Y., Wen, L., and Lyu, S. Stochastic online auc maximization. In *NIPS*, pp. 451–459, 2016.
- Zadrozny, B., Langford, J., and Abe, N. Cost-sensitive learning by cost-proportionate example weighting. In *Third IEEE international conference on data mining*, pp. 435–442. IEEE, 2003.
- Zhao, P., Hoi, S. C., Jin, R., and YANG, T. Online auc maximization. 2011.